Particle Bombardment as Viewed by Molecular Dynamics

Barbara J. Garrison

Department of Chemistry, The Pennsylvania State University, University Park, PA 16802

A classical dynamics model is used to investigate nuclear motion in solids due to bombardment by energetic atoms and ions. Of interest are the mechanisms of ejection and cluster formation both of elemental species such as Ni_n and Ar_n and molecular species where we have predicted intact ejection of benzene-C_6H_6, pyridine-C_5H_5N, napthalene-$C_{10}H_8$, biphenyl-$C_{12}H_{10}$ and coronene-$C_{24}H_{12}$. The results presented here show that the energy distributions of the parent molecular species, e.g. benzene, are narrower than those of atomic species, even though the ejection processes in both cases arise from energetic nuclear collisions. The bonding geometry also influences the ejection yield and angular distribution. The specific case of π-bonded and σ-bonded pyridine on a metal surface is discussed with comparisons between the calculated results and experimental data.

The bombardment of solids by energetic particle beams has attracted interest due to the ejection of large and novel species. These species can be molecules that are present in the original sample such as a dodecanucleotide (1) or clusters that are formed during the bombardment event, for example $[NO(N_2O_3)_3]^+$ ejected from solid nitrous oxide (2). Numerous other examples appear in these proceedings.

Our goal has been to understand the ejection mechanisms and the relationship of the clusters to the original configuration of atoms in the sample. Many mechanisms involving both the motion of the atomic nuclei and/or of electrons can be proposed to be responsible for ejecting the molecules. However, if a solid (or liquid) sample is bombarded by a heavy particle with energy in the 100-10000 eV range there must be energetic collisions between the atomic nuclei.

0097-6156/85/0291-0043$06.00/0

Thus as a starting point for understanding the bombardment process we have developed a classical dynamics procedure to model the motion of atomic nuclei. The predictions of the classical model for the observables can be compared to the data from sputtering, spectrometry (SIMS), fast atom bombardment mass spectrometry (FABMS), and plasma desorption mass spectrometry (PDMS) experiments. In the circumstances where there is favorable agreement between the results from the classical model and experimental data it can be concluded that collision cascades are important. The classical model then can be used to look at the microscopic processes which are not accessible from experiments in order to give us further insight into the ejection mechanisms.

Briefly, the theoretical model consists of approximating the solid and possible adsorbed molecules by a finite array of atoms (3-12). Assuming a pairwise interaction potential among all the atoms, Hamilton's equations of motion are integrated to yield the positions and momenta of all particles as a function of time during the collision cascade. The final positions and momenta can be used to determine the experimental observables such as total yield of ejected particles, energy distributions, angular distributions and possible cluster formation. One advantage of the classical procedure is that one can monitor the collision events and analyze microscopic mechanisms of various processes.

Mechanisms of Cluster Formation

From the classical dynamical treatment, it is possible to examine the cluster formation mechanism in detail and to provide semiquantitative information about cluster yields. In general, these calculations suggest that there are three basic mechanisms of cluster formation (12). First, for systems with atomic identity such as metals, or atomic adsorbates on a solid, the ejected atoms can interact with each other in the near-surface region above the crystal to form a cluster by a recombination type of process (3-5). This description would apply to clusters of the type M_nO_m observed in many types of SIMS experiments. In this case the atoms in the cluster do not need to arise from contiguous sites on the surface, although in the absence of long-range ionic forces the calculations indicate that most of them originate from a circular region of radius ~ 5 angstroms. This rearrangement, however, complicates any straightforward deduction of the surface structure from the composition of the observed clusters. We have observed an Ar_{25} cluster to eject from solid argon via this mechanism (13). We would also speculate that the alkali halide clusters $(CsI)_nCs^+$ with n as large as 70 (14) also form by this basic mechanism.

A second type of cluster emission involves molecular species which can be as simple as carbon monoxide or as complicated as the dodecanucleotide mentioned above. In the first case, the CO bond strength is ~ 11 eV, but the interaction with the surface is only about 1 eV. Calculations indicate that this energy difference is sufficient to allow ejection of CO molecules, although ~ 15 percent of them can be dissociated by the ion beam or by energetic metal atoms (6). For such molecular systems it is easy to infer the original atomic configurations of the molecule and to determine the

surface chemical state. If CO were dissociated into oxygen and carbon atoms, for example, the calculations suggest that the amount of CO observed should drop dramatically.

Although the basic principles behind this intact ejection mechanism can be illustrated with carbon monoxide, the extrapolation to large bioorganic molecules is not necessarily obvious. Calculations have been performed for a series of organic molecules adsorbed on a Ni(001) surface to understand the mechanisms of molecular ejection (8-12). The first molecules which have more than just a few atoms examined are benzene which π-bonds on a metal surface and pyridine which can either π-bond or σ-bond on a metal surface. Larger structures, whose sizes approach the diameter of bioorganic molecules, are naphthalene, biphenyl and coronene whose adsorption structures are unknown. All the molecules except pyridine are assumed to π-bond on the surface.

In all cases we find that the molecular species may be ejected intact. From our theoretical calculations, three factors favor this process (8-9). First, a large molecule has many internal degrees of freedom and can absorb energy from an energetic collision without dissociating. Second, in the more massive framework of a large organic molecule, individual atoms will be small in size compared to a metal atom; thus, it is possible to strike several parts of the molecule in a concerted manner so that the entire molecule moves in one direction. Finally, by the time the organic molecule is struck, the energy of the primary particle has been dissipated so that the kinetic energies are tens of eVs rather than hundreds or thousands of eVs. These three factors are equally valid for the ejection of either carbon monoxide, benzene or coronene. However, in the cases of the larger molecules, we found that often 2-3 metal atoms would strike different parts of the molecule during the ejection process. The time for the molecules to eject after the primary particle has hit the sample is less than 200 femtoseconds (fs; $1 fs = 1 \times 10^{-15} s$). This intact ejection mechanism for molecules can be applied to molecular solids. We find for the bombardment of ice shows that the water molecules also eject intact (15).

It is difficult to make quantitative determinations of the fragment yields because the forces that govern all the rearrangement channels are not known. However, there is one interesting feature related to fragmentation that we have observed. Most of the fragments formed from direct collisions within ~ 0.2 ps are the parent molecule minus an H, CH, or C_2H_2. These arise from an energetic collision that rips off part of the molecule. In the case of biphenyl however, a severing between the two rings is observed to occur with some frequency. Thus the structure of the molecule influences the nature of the direct fragmentation process. These small CH type species will undoubtedly be formed during the ion bombardment process. To be detected, however, in a conventional SIMS or FABMS apparatus they must be formed as an ion. Within this classical model we are unable to predict the charge fraction.

The final mechanism for cluster ejection is essentially a hybrid mechanism involving both intact ejection and recombination. In the case of CO on Ni_3Fe, we find that the observed NiCO, Ni_2CO

and NiFeCO clusters form by a recombination of ejected Ni and Fe atoms with ejected CO molecules. There is apparently no direct relation between these moieties and linear and bridge-bond surface states. In the case of cationized species such as $NiC_6H_6^+$ ions, we propose a reaction of the type

$$Ni^+ + C_6H_6 \xrightarrow[\text{surface}]{} NiC_6H_6^+ \qquad (1)$$

The presumption that the Ni supplies the charge is based on the fact that no $C_6H_6^+$ is observed (16) and that the ionization potential of Ni is less than that of benzene.

This final hybrid mechanism may be responsible for the formation of the dimer ion of the dodecanucleotide (1) or of water clusters (17). Each molecular unit ejects intact and then interacts with other molecules in the near surface region to form the cluster entities. In the case of $(H_2O)_2$ clusters our calculations indicate that the two H_2O molecules originate from mostly adjacent sites on the surface (15). This is a consequence of the relatively weak H_2O-H_2O interaction. Ionic clusters such as $(H_2O)H^+$, however, can form from an H_2O molecule and an H^+ ion that were further apart on the surface.

The fact that the composition of the ejected clusters may be different from the original arrangement of surface atoms is somewhat discouraging. As it turns out, however, there are situations where the precise nature of the rearrangement can be predicted theoretically. One example involves the measured O_2^-/O^- ratio as a function of oxygen coverage on Ni(001). This ratio is four times higher for 50 percent oxygen coverage [c(2x2)coverage] than for 25 percent oxygen coverage [p(2x2)surface], a change that is also calculated with the model (18). The reason for this effect is that there are no closely neighboring oxygen atoms on the p(2x2) surface, and the O_2 formation probability is much lower. Concepts of this sort may be useful in testing for island-growth mechanisms and distinguishing them from those that proceed through several distinct phases.

Energy Distributions

The energy distribution of atomic species ejected in bombardment experiments are characterized by a peak at 1-5eV and a high energy tail that goes approximately as E^{-n} where $n \approx 2$. This distribution is characteristic of a non-equilibrium collision cascade. The energy distributions of the parent molecular species are much narrower, however, and often terminate at ~10eV. Shown in Figure 1a are experimental energy distributions for Ag^+, $C_6H_5^+$ and $C_2H_2^+$ ions ejected from a system with a monolayer of benzene adsorbed on a Ag(111) crystal face (19). Since the molecular species is ejecting during the same collision cascade as the Ag^+ ions and on the same timescale one would expect the distribution of collision energies that cause ejection to be the same for the Ag atoms and

the C_6H_6 molecules. However, the energetic collisions with the molecular species can and do cause fragmentation. Thus the energetic benzene molecules are depleted. The fragments then should have a distribution at higher energies as is illustrated by the $C_2H_2^+$ fragment energy distribution shown in Figure 1a. Note that the peak of the $C_2H_2^+$ distribution is at a higher energy than that of the $C_6H_5^+$ distribution. Since the peak position can be correlated to the binding energy of the species to the surface, the peak of the $C_2H_2^+$ distribution should be higher since its binding energy includes two C-C bond energies. The energy distributions from the calculations (Figure 1b) illustrate the same physical phenomena.

It is tempting to use the energy distributions of the ejected particles as a key to understanding the mechanisms responsible for the desorption. Care must be taken, however, as collision cascades can give rise to at least three distinctive shapes of energy distributions as shown in Figure 1. (The calculations also predict the distribution of metal atoms to have a high energy tail.) In fact the calculated C_6H_6 distribution of Figure 1b can be reasonably approximated by a Maxwell-Boltzmann form even though a thermal equilibrium is not present in the solid during the ejection event. The calculations indicate that energy distributions of elemental (and preferably both the neutral and charged) species could possibly be the most useful for comparing to the different experimental mechanisms as these particles cannot be fragmented in energetic collisions. Even here, however, one can obtain energy distributions from SIMS experiments that fall off more rapidly than E^{-2} if low energy (<250 eV) primary ion beams are used (20).

Matrix Effects

The composition of the solid or matrix which is being bombarded has a large influence on the types of species observed to eject. This is true not only for the ionization process but also for the nuclear motion. Shown in Figure 2 are SIMS spectra of benzene taken for three different substrates. The data in Figure 2b was obtained for Ar^+ ion bombarded Ni(001) exposed to 3 langmuirs of benzene (16). This dose corresponds to approximately one monolayer coverage. This spectrum contains only the Ni^+, Ni_2^+ and $NiC_6H_6^+$ ions. Karwacki and Winograd also performed SIMS experiments for C_6H_6 adsorbed on Ni(001) where they dosed the surface with 2100 langmuirs of benzene (16). This SIMS spectrum is shown in Figure 2c. Here the multiple layers of benzene attenuate the Ni^+, Ni_2^+, and cationized $NiC_6H_6^+$ peaks. This spectrum, however, does contain hydrocarbon fragments of lower masses.

Two SIMS experiments have been performed on solid benzene at a temperature of 77 K (17,21). The mass spectrum from Lancaster et al. is shown in Figure 2d. They observe peaks at all masses corresponding to $C_nH_m^+$ where $n \leq 30$. The predominant peaks are the C_1, C_2, and C_3 species, in agreement with the work of Karwacki and Winograd (Figure 2c). We believe the reason we do not observe these $C_nH_m^+$ species with $n > 6$ in the calculations is due to the low density of benzene molecules on the Ni surface.

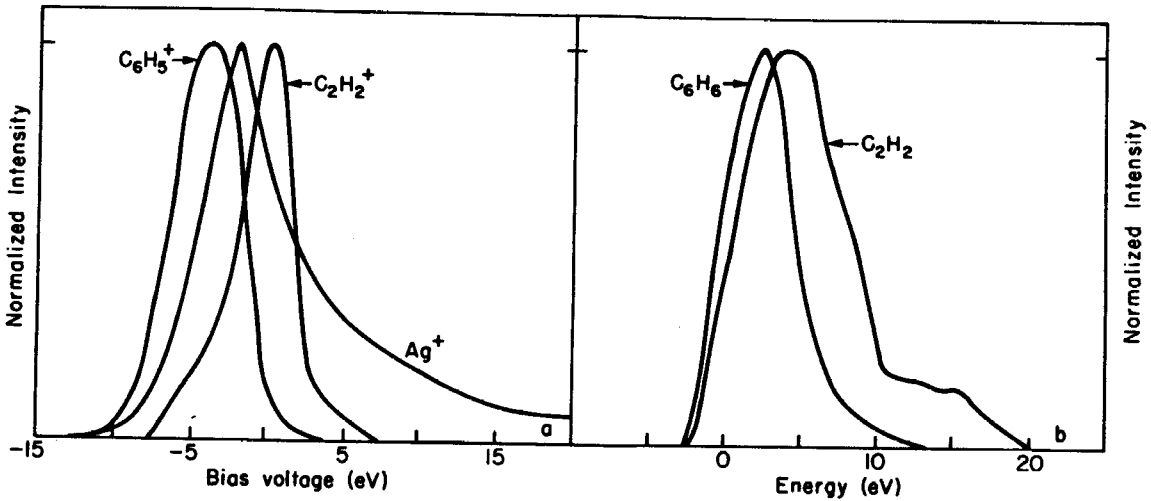

Figure. 1. Energy Distributions. a) Experimental Ag^+, $C_6H_5^+$ and $C_2H_2^+$ ion intensities from one monolayer of benzene adsorbed on Ag(111) plotted versus the voltage on the sample. The primary particle is Ar^+ with energy 1 keV incident on the sample at a polar angle of 45°. The secondary particles are collected at a polar angle of 60°. The raw data has been smoothed. This data has been graciously provided by D. W. Moon, R. J. Bleiler and N. Winograd prior to publication. b) Calculated C_6H_6 and C_2H_2 energy distributions from one monolayer of benzene on Ni(001). All ejected particles have been counted. The energy resolution is 5eV. The calculations are described in ref. 9. Reproduced with permission from Ref. 12.

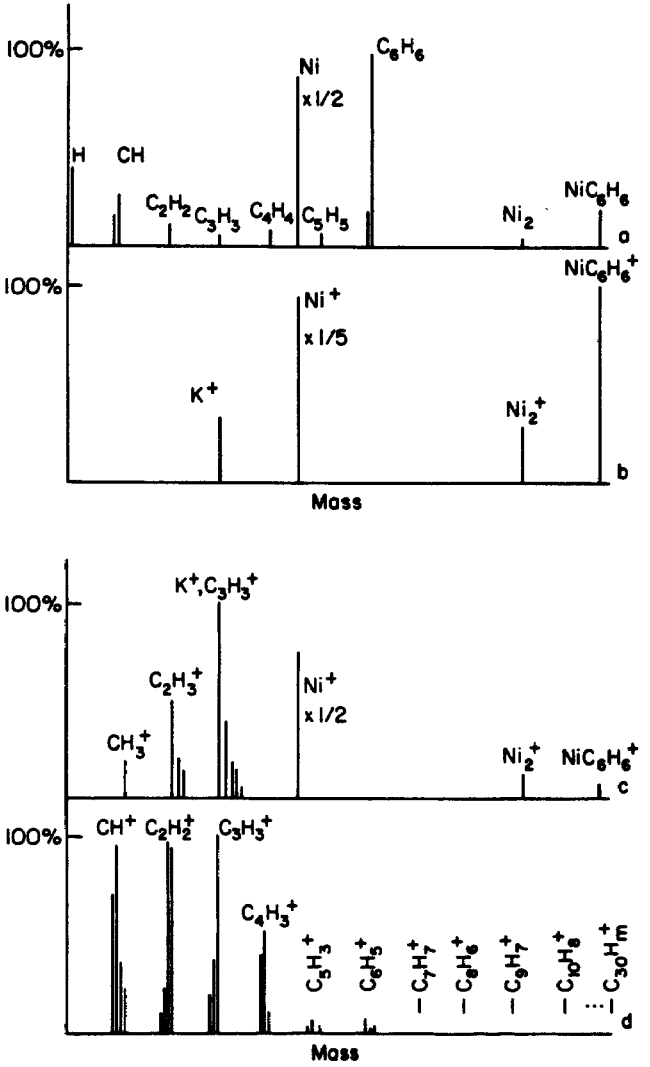

Figure 2. Benzene mass spectra. The most intense peak in each grouping has been identified. a) Calculated, (9). b) Experimental SIMS, 3 langmuirs of C_6H_6 on Ni(001), (16). c) Experimental SIMS, 2100 langmuirs of C_6H_6 on Ni(001), (16). d) Experimental SIMS, solid benzene (17). Reproduced with permission from Ref. 12. Copyright 1983, Elsevier Science Publishing Co.

It is obvious from Figure 2b-d that the sample preparation strongly affects the mass spectrum. The low coverage study appears to be the one where the parent species can be most easily identified as long as there is an energetically favorable means of ionization, e.g., cationization. The solid benzene studies are interesting in that a variety of large clusters are observed. However, if the sample were of an unknown compound, it would be difficult to extract the parent species from Figure 2d. The calculated spectrum (Figure 2a) predicts the parent molecule, C_6H_6, to be the most abundant organic species. The comparable experimental data, Figure 2b, however, has no $C_6H_6^+$ peak but a large $NiC_6H_6^+$ peak. Here then, the electronic environment influences which species are observed.

Molecular Orientation Effects: Benzene vs. Pyridine

It is of interest to compare the ejection mechanisms for molecules bonded to the surface with different orientations. In benzene, the interaction with the surface is shared among six carbon atoms via the π-electron cloud. In pyridine, however, the bonding occurs almost totally through the nitrogen atom while the remainder of the molecule is pointing away from the surface. The most striking difference between the two cases is that the computed yield of molecular species for the pyridine system is extremely low (9). The reasons for the major difference in yields for these two structures is clear from an analysis of the trajectories that lead to molecular ejection of pyridine. Very simply, pyridine ejection requires the specific cleavage of a N-Ni bond during a single collision. When a carbon atom is struck, the molecule either stays on the surface or tends to dissociate. There appears to be no efficient modes of transferring the energy of collisions with the molecule into translation away from the surface. Obviously the original structure of the organic molecules, then, affects the ejection and fragmentation processes. One would not necessarily expect similar spectra from a sample of a monolayer of organic molecules on a metal, a liquid, or an ordered solid.

These orientational effects have recently been confirmed in SIMS measurements of pyridine and benzene adsorbed on Ag(111) (22). In this system the benzene π-bonds to the surface while the pyridine π-bonds at low coverages but rearranges at higher coverages to σ-bond to the surface. The intensity of the $AgC_6H_6^+$ ion monotonically increases as the benzene coverage on the silver surface is increased to one monolayer. The $AgC_5H_5N^+$ and $C_5H_5NH^+$ ion intensities, however, initially increase and then decrease as the molecule rearranges on the surface, and finally increase again as the pyridine coverage is increased to one monolayer.

The arrangement of the molecules on the surface also influences the angular distributions of the ejected species (22). The polar angle distributions of various ejected ions for four systems ~2.5 L benzene (monolayer), 4.5 L pyridine (monolayer, σ-bonded) 0.15 L pyridine (π-bonded), and 12 L thiophene (monolayer) on Ag(111) have been measured. The results of these distribution measurements are illustrated in Figure 3. For

monolayer benzene and for low coverage pyridine where the molecules are believed to lie flat on Ag(111), the polar angle distribution of $(M-H)^+$ (benzene) and $(M+H)^+$ (pyridine) are broad with a peak at $\theta = 20°$ measured with respect to the surface normal. At the onset of the change in bonding configuration, however, the polar angle distribution of the $C_5H_5NH^+$ ion sharpens dramatically and the peak moves to $\theta = 10°$. It appears that the array of σ-bonded pyridine molecules provides a means of focusing the direction of ejection of the pyridine molecules. Further, the polar angle distribution of the high kinetic energy ions (6-10eV) ejected from the σ-bonded pyridine structure is 20-30% wider than the distribution of the low kinetic energy ions (3-7eV) as is shown in Figure 1b. This trend toward wider polar angle distributions for faster moving particles is counter to that observed for atom ejection. The polar angle distribution of thiophene, is narrow with a peak at $\theta = 10°$C, indicating that it also is σ-bonded to the surface.

In this case it appears that the σ-bonded pyridine molecules are channeling the ejecting pyridine molecules into the vertical direction (23). One example of how this blocking can significantly affect the trajectory of an ejecting pyridine molecule is illustrated in Figure 4. Only the species (one Ar^+ ion and two pyridine molecules) directly involved in this particular ejection process are shown. In this example the metal substrate plays no direct role in ejecting the molecule. The grid lines are drawn between the nearest-neighbor atoms in the first plane of the microcrystallite. The elapsed time during the collision process is shown in fs (1 fs=1x10^{-15} s). The initial positions of the atoms are drawn in Figure 2 (0 fs). At 33 fs the Ar^+ ion, which has backscattered from the surface, is colliding with 3 carbon atoms i the target pyridine molecule. The kinetic energy of the center of mass of this pyridine molecule is 11.6 eV and its molecular axis is oriented at a polar angle of θ=66° from the surface normal. At 85 fs the ejecting pyridine molecule collides with a neighboring pyridine molecule and dissipates a fraction of its momentum. At the final stage of the sputtering process (120 fs), the pyridine molecule ejects molecularly, even though distorted, at a polar angle of θ=31° with 1.40 eV of kinetic energy. Due to the blocking by a neighboring pyridine molecule, the polar angle of the ejected pyridine molecule is altered from 66° to 31°. The walls created by pyridine molecules are not completely rigid as indicated by the distorted molecule shown on the left in the 120 fs frame. Therefore, a pyridine molecule ejecting with a large kinetic energy will not feel a strong enough force to channel it completely into the upward direction. The polar angle distribution of the high energy ejected particles is thus broader than that of the low energy ejected particles. This mechanism is distinct from that found with atom ejection. In this latter case, the energy dependence of the azimuthal distribution is related to the time of ejection and consequently to the amount of surface structure present when the atom ejects. Note that for the π-bonded benzene system, there are no channels to orient the ejecting molecules.

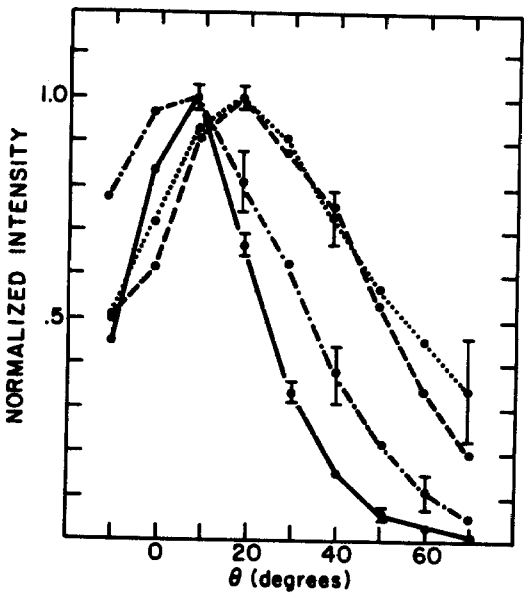

Figure 3. Normalized polar angle distribution of molecular ion yields for 4.5 L pyridine (——, $(M+H)^+$), 0.15 L pyridine (----, $(M+H)^+$), 2.5 L benzene (····, $(M-H)^+$), and 12 L thiophene (—·—·— —·—, M^+) on Ag(111) at 153K. The pyridine and benzene data is from (22) and thiophene data has been supplied by the same authors.

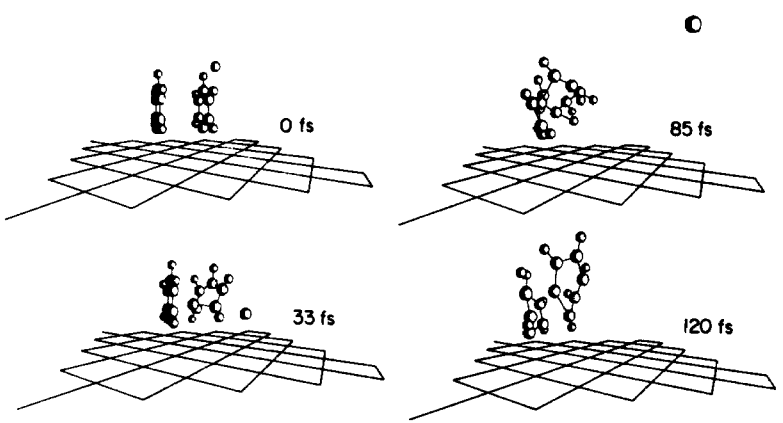

Figure 4. Change of the ejection angle of a sputtered pyridine molecule (right one) due to the blocking by a neighboring pyridine molecule (left one). The labels are in fs where 1 fs = $1x10^{-15}$ second. (0 fs) Initial positions of the atoms. (33 fs) The backscattered Ar^+ ion collides and ejects the pyridine molecule at a polar angle of θ=66°. (85 fs) The ejecting pyridine molecule is blocked by a neighboring pyridine molecule. (120 fs) Finally, the ejection polar angle is changed to θ=31°. Both the sputtered molecule and the blocking molecule are distorted. Reproduced with permission from Ref. 23. Copyright 1985, Elsevier Science Publishing Co.

Fragmentation

There has been considerable speculation as to whether the observed fragments form primarily from direct collisions at the surface (i.e. within $\sim 0.2 \times 10^{-12}$s after the primary particle has struck) or from dissociation of larger species during the flight to the detector (often as long as 10^{-4}s). The calculations show that it is definitely possible to form numerous fragments in direct collisions at the surface (Figure 2a). From the calculations we have estimated that approximately three quarters of the ejected benzene molecules have less than 5 eV of internal energy (9). There is a reasonable probability that these vibrationally colder molecules will remain intact. The energetic molecules, on the other hand, will undoubtedly dissociate.

At this stage it is necessary to design clever experiments or theoretical approaches to help elucidate the different possible modes of fragmentation. Recently Moon (24) has proposed a method of examining the polar angle distributions as a means of differentiating between the fragmentation schemes. He finds that for chlorobenzene adsorbed on Ag(111) that the $C_6H_5^+$ and Cl^- ions probably form by direct collisions on the surface. For the chlorobenzene as well as benzene and pyridine adsorbed on silver, he found that neither molecular or fragment ions formed by gas phase decomposition of a cationized species.

In the case of the alkali halide clusters (14), recent work has shown that the oscillations in ion intensity with cluster size are due to dissociation of metastable species during the flight to the detector (25). Spectra taken 0.2μs after bombardment exhibit a monotonic decrease in ion intensity with increasing cluster size. Spectra taken after 70μs, however, show an increase in the $(CsI)_{13}Cs^+$ ion intensity and a decrease in the $(CsI)_{14}Cs^+$ and $(CsI)_{15}Cs^+$ ion intensities. Here then, decomposition of larger species during the flight to the detector has a noticeable effect on the cluster yields. These experiments though make no statement as to how the clusters are initially formed near the surface.

Closing Statements

A classical dynamics model has been developed to investigate the importance of collisional processes in heavy particle bombardment experiments. This procedure is very powerful for describing collisional events and provides a working hypothesis against which experimental data can be compared. We have shown numerous examples from SIMS experiments where the calculations have fit experimental data very well. The time has come for the experimentalists to conceive and execute experiments aimed at uncovering the fundamental processes involved in the SIMS and FABMS procedures.

It should be noted that various researchers have different goals for using and understanding the ion bombardment process. There are those who are using the technique to obtain information about a molecule that they have placed on the surface. That is, they want a mass and possibly a structure determination. Other researchers are primarily concerned with determining the elemental composition of the sample while others use the technique to measure

the geometrical arrangement of the atoms and molecules on the surface. Another area of interest is to probe the electronic processes involved when an atom or molecule is in the near surface region. Although these goals are quite varied the fundamental processes are intermingled. To understand our own area of interest we need to understand all of the experimental results and the detailed events occurring on the microscopic level.

Acknowledgment

The interaction with those who have supplied the experimental data, D. W. Moon, R. J. Bleiler, E. J. Karwacki and N. Winograd, has greatly helped in solidifying many of the ideas presented here. I thank them for allowing me to use their data as well as for many stimulating conversations. The financial support of the National Science Foundation, the Office of Naval Research and the Camille and Henry Dreyfus Foundation is gratefully acknowledged.

Literature Cited

1. McNeal, C. J.; Macfarlane, R. D. J. Am. Chem. Soc. 1981, 103, 1609.
2. Orth, R. G.; Jonkman, H. T.; Michl, J. J. Am. Chem. Soc. 1981, 103, 1564.
3. Garrison, B. J.; Winograd, N.; Harrison Jr., D. E. J. Chem. Phys. 1978, 69, 1440.
4. Winograd, N.; Harrison Jr., D. E.; Garrison, B. J. Surface Science 1978, 78, 467.
5. Garrison, B. J.; Winograd, N.; Harrison Jr., D. E. Phys. Rev. B 1978, 18 6000.
6. Winograd, N.; Garrison, B. J.; Harrison Jr., D. E. J. Chem. Phys. 1980, 73, 3473.
7. Foley, K. E.; Garrison, B. J. J. Chem. Phys. 1980, 72, 1018.
8. Garrison, B. J. J. Am. Chem. Soc. 1980, 102, 6553.
9. Garrison, B. J. J. Am. Chem. Soc. 1982, 104, 6211.
10. Garrison, B. J. J. Am. Chem. Soc. 1983, 105, 373.
11. Winograd, N.; Garrison, B. J. Accts. of Chem. Res. 1980, 13, 406.
12. Garrison, B. J.; Winograd, N. Science 1982, 216, 805; Garrison, B. J. Int. J. Mass Spec. and Ion Phys. 1983, 53, 243.
13. Garrison, B. J.; Winograd, N. Chem. Phys. Lett. 1983, 97, 381.
14. Barlak, T. M.; Wyatt, J. R.; Colton, R. J.; Decorpo, J. J.; Campana, J. E.; Campana, J. E.. J. Am. Chem. Soc. 1982, 104, 1212.
15. Brenner, D. W.; Garrison, B. J. unpublished results.
16. Karwacki, E. J.; Winograd, N. Anal. Chem. 1983, 55, 79.
17. Lancaster, G. M.; Honda, F.; Fukuda, Y.; Rabalais, J. W. J. Am. Chem. Soc. 1979, 101, 1951.
18. Winograd, N.; Garrison, B. J.; Fleisch, T.; Delgass, W. N.; Harrison Jr., D. E. J. Vac. Sci. Tech. 1979, 16, 629.
19. Moon, D. W.; Bleiler, R. J.; Winograd, N. unpublished results.